

The First and Second Order Statistics of Beam Wave Pulses Backscattered from Aperiodic Surfaces with Application to Satellite Altimetry

Mitsuo Tateiba and Tetsushi Takegawa

Department of Computer Science and Communication Engineering
 Kyusyu University
 6-10-1 Hakozaki, Higashi-ku, Fukuoka 812, JAPAN

1. Introduction

The satellite altimeter, one of microwave active sensors, is basically the short pulse monostatic radar ^{1),2)}. The radar is pulse limited when the transmitted pulsewidth is short enough that the entire ocean target within the antenna beam is not simultaneously illuminated. The radar pulses are transmitted toward the ocean surface successively at a pulse repetition frequency. In existing satellite altimeters, the ocean surface measurement is limited only to the ocean waveheight by analyzing the leading edge of the mean return waveform of pulses backscattered from the ocean surface; besides, pointing errors (off-nadir angles) are determined by the analysis of the trailing edge. The basic idea behind the measurement is that if the ocean surface may be regarded as the ensemble of statistically independent scatterers then the mean power received on satellite is expressed as the sum of powers backscattered from each scatterer ^{3),4)}. Therefore, only the first order statistics of received pulses has been used up to now ²⁾.

To measure other ocean surface state parameters such as the wavelength and the roughness and to increase the accuracy of existing measurements are the center of interest in satellite altimetry. We consider that a standard method of studying the fundamental subject is to use the higher order statistics as well as the first and/or to make more clear the pulse scattering from ocean surfaces. Then, in the previous paper ⁵⁾, the spherical wave pulse train backscattered from aperiodic surfaces was simulated with good approximation by the application of an improved method of stationary phase, and it was shown that the pulse train has the statistical property similar to that of the practical pulses received by altimeters. However, the directional property of the antenna has been taken into no account.

In this paper, the beam pulses backscattered from aperiodic surfaces are simulated by the same method and some of the characteristics of the first and second statistics of the pulses are shown graphically; in particular, it is emphasized that the effect of off-nadir angles is of importance on the wavelength measurement based on the first statistics only.

2. Beam Wave Pulses Backscattered from Aperiodic Surfaces

Consider the two-dimensional backscattering of microwave beams from a conducting surface $h(x)$, as shown in Fig. 1. The incident wave, which is the z component of the electric field, is assumed to be on the surface

$$U_i(r) = j \frac{4\sqrt{\pi k^2 Z_0^2 \ln 2}}{\theta_0^2} D(\theta) H_0^{(1)}(kr) \quad D(\theta) = \exp\left\{-\ln 2 \frac{(\theta - \alpha)^2}{2\theta_0^2}\right\} \quad (1)$$

where $k = \omega\sqrt{\epsilon_0\mu_0}$ is the wavenumber in free space, $Z_0 = \sqrt{\mu_0/\epsilon_0}$ is the intrinsic impedance of free space, $H_0^{(1)}$ is the Hankel function of the first, of order 0,

and $D(\theta)$ indicates the directional property of the satellite antenna with the beamwidth $2\theta_0$ in which the pointing error α is assumed. Here, the radiation power of $u_i(r)$ is normalized to be 1(W). The following parameters are assumed: the mean altitude $\rho=800$ (km), $2\theta_0=1.5^\circ$, the frequency $\omega/2\pi=13.9$ (GHz) and the pulsewidth $\tau=3$ (ns).

We pay attention only to ocean surfaces without fine undulation, so that $h(x)$ is assumed to be an aperiodic (almost periodic) function ⁶⁾.

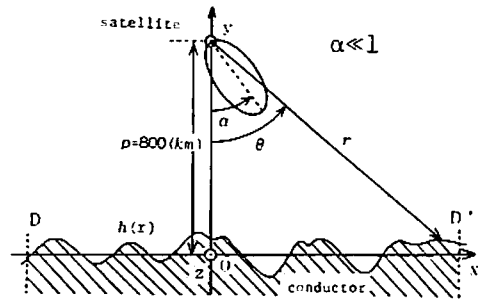


Fig.1 Geometry of Problem.

$$h(x) = a_1 \sin(2\pi \frac{x}{\lambda_1} + 0.78) + a_2 \sin(2\pi \frac{x}{\lambda_2} + 1.6) + a_3 \sin(2\pi \frac{x}{\lambda_3} + 2.40) + a_4 \sin(2\pi \frac{x}{\lambda_4} + 0.4) \quad (2)$$

As a typical example of calm seas, $a_1=0.5$, $a_2=0.25$, $a_3=0.1108$, $a_4=0.0625$, $\lambda_1=200.0$, $\lambda_2=10.95$, $\lambda_3=6.28$, $\lambda_4=4.795$ (m) are assumed, where the significant waveheight (SWH) is 0.7(m) and the significant wavelength (SWL) is 10.95(m). The previous paper ⁵⁾ shows that the physical-optics approximation and the improved method of stationary phase are valid for the present analysis. Therefore, the z component of the received electric field can be expressed as

$$U_s = \frac{-\sqrt{2kZ_0\pi \ln 2}}{\pi\rho\theta_0} \sum_{i=1}^N \sqrt{\frac{\pi}{k|r^{(2)}(x_i)|}} f(x_i) \{D(\theta_i)\}^2 \exp\{j2kr(x_i) \pm j\frac{\pi}{4}\} \\ + \frac{-\sqrt{2kZ_0\pi \ln 2}}{\pi\rho\theta_0} \sum_{i=1}^{N_i} \{D(\theta_{ai})\}^2 \int_{x_{ai}-\Delta x_i}^{x_{ai}+\Delta' x_i} f(x) \exp\{j2kr(x)\} dx \quad ; \quad (3)$$

$$f(x) = \{\rho - h(x) + \lambda h^{(1)}(x)\} / r(x) \quad r(x) = \sqrt{x^2 + \{\rho - h(x)\}^2}$$

where x_i denotes a stationary point (SP) and is a root of $r^{(1)}(x_i)=0$, the sign \pm in the exponential depends on $r^{(2)}(x_i)=d^2r(x)/dx^2|_{x=x_i} \geq 0$, x_{ai} is a point of inflection (IP) satisfying $2k|r^{(1)}(x_{ai})| < 10$ (rad/m), $\theta_i = \tan^{-1}\{x_i / \{\rho - h(x_i)\}\}$, $\theta_{ai} = \tan^{-1}\{x_{ai} / \{\rho - h(x_{ai})\}\}$, $h^{(1)} = dh(x)/dx$, and $\Delta' x_i$, Δx_i are properly determined.

The received pulse $u_s(t)$ is given by multiplying (3) by the spectral function of the incident rectangular pulse and then by taking the inverse Fourier transform. The pulse scattered from the SP keeps the waveform before scattering, while the IP scattering deforms the waveform. Because the waveform deformation is not so large and the number of SP is much greater than that of IP, the deformation due to the IP scattering is small in the entire waveform. Then we can readily obtain the inverse transform.

3. The First Statistics of Received Pulses

Because the pulses are transmitted at a pulse repetition frequency $1/\Delta t$, the mean return waveform (MRW) is expressed in terms of the received pulse $u_s(t)$ as follows:

$$P(t) = \frac{1}{n} \sum_{k=1}^n p_k(t) \quad ; \quad p_k(t) = \frac{[Re\{U_s(t)\}]^2}{Z_0} \quad (4)$$

where $p_k(t)$ is the k th return waveform and Re stands for the real part. Figure 2 shows the MRWs of beam wave pulses (dotted line) and spherical wave pulses (solid line), and shows that there is hardly any difference between two curves. However, when the pointing error occurs, the MRW changes with the off-nadir angle as well known¹⁾. In addition, it depends on the sea state. Each MRW for calm and moderate seas is shown in Figs. 3 and 4, respectively, where all the peak values of the MRWs for the off-nadir angles are normalized to be 1. If not normalized, the MRWs change as shown in Fig. 5 and the change of the trailing edge becomes remarkable even for calm seas.

4. The Second Statistics of Received Pulses

Both deviations of the i th return pulse from the MRW and of the i th return pulse when transmitted with time lag t_c , respectively, are expressed by

$$q_i(t) = p_i(t) - \frac{1}{n} \sum_{i=1}^n p_i(t), \quad q_{i,t_c}(t) = p_{i,t_c}(t) - \frac{1}{n} \sum_{i=1}^n p_{i,t_c}(t).$$

Then the correlation coefficient of $q_i(t)$ and $q_{i,t_c}(t)$ may be defined⁷⁾ by

$$C(t) = \left\{ \frac{1}{n} \sum_{i=1}^n q_i(t) q_{i,t_c}(t) \right\} / \sqrt{ \frac{1}{n} \sum_{i=1}^n \{q_i(t)\}^2 \cdot \frac{1}{n} \sum_{i=1}^n \{q_{i,t_c}(t)\}^2 } \quad (5)$$

where the train $\{p_i(t)\}$ can be treated as independent pulses series because the time difference Δt between $p_i(t)$ and $p_{i+1}(t)$ is assumed to be 5(ms).

Figures 6 and 7 show that the correlation coefficient is independent of the directional property of the antenna. Let us examine the effect of the ocean wavelength on the MRW and the correlation coefficient. When the ocean waveheight is constant and the wavelength is variable, the MRW has the same rise time and the peak power decreases as the wavelength becomes short (Fig. 8), while the correlation coefficient is independent of the wavelength (Fig. 9). It should be noted that the change of the MRW with the ocean wavelength is similar to that with the off-nadir angle (see Figs. 5 and 8). Finally we assume periodic surfaces. In this case it can be shown that the MRW is quite deformed and the waveheight can not be determined by the analysis of the leading edge of the MRW; of course, the correlation between return pulses is strong.

5. Conclusion

The first and second statistics of beam wave pulses backscattered from aperiodic surfaces are shown graphically and similar to that of actual pulses received by satellite altimeters. Because the simulated pulse train is a raw scattering data before processing, it is useful for studying new measurement of ocean surfaces and the increase of the accuracy of existing measurements.

Acknowledgment This work was supported in part by Scientific Research Grant-In-Aid (grant 59550233, 1984) from the Ministry of Education, Science, and Culture, Japan.

REFERENCES

- 1) J.T. McGoogan, IEEE Trans., Microwave Theory Tech., MIT-23, 970 (1975).
- 2) Report of TOPEX Science Working Group, Jet Pro. Lab., Cal. Inst. Tech. (1981).
- 3) R.K. Moore and C.S. Williams, Jr., Proc. IRE, 45, 228 (1975).
- 4) T. Berger, IEEE Trans., Antennas Propagat., AP-20, 295 (1972).
- 5) M. Tateiba, Proc. 1984 Int. Symp. on Noise and Clutter Rejection in Radars and Imaging Sensors, 217 (1984).
- 6) R.R. Lentz, Radio Sci., 9, 1139 (1974).
- 7) E.J. Walsh, *ibid.*, 17, 786 (1982).

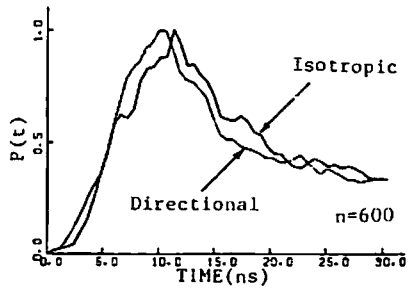


Fig. 2 The Mean Return Waveforms of Pulses Received by the Directional and Isotropic Antennas.

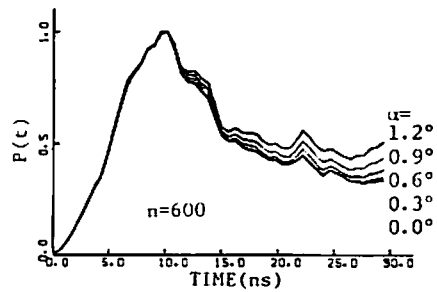


Fig. 3 The Normalized Mean Return Waveforms of Pulses Received at the Off-Nadir Angles for a Calm Sea.

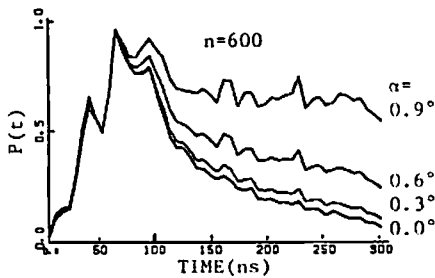


Fig. 4 The Normalized Mean Return Waveforms of Pulses Received at the Off-Nadir Angles for a Moderate Sea.

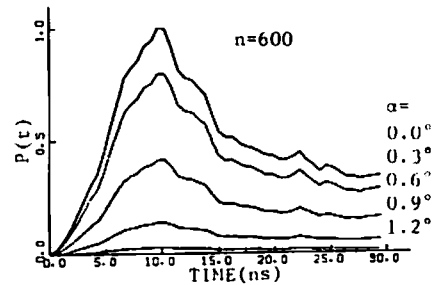


Fig. 5 The Mean Return Waveforms of Pulses Received at the Off-Nadir Angles for a Calm Sea (Another Expression of Fig. 3).

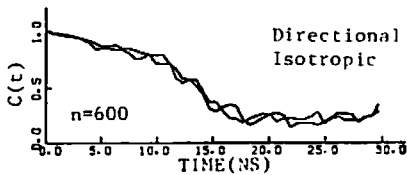


Fig. 6 The Correlation Coefficients of Return Pulses Received by the Directional and Isotropic Antennas.

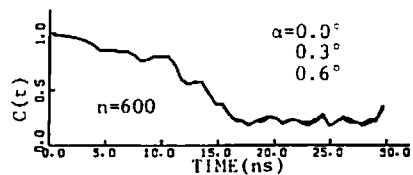


Fig. 7. The Correlation Coefficients of Return Pulses Received at the Off-Nadir Angles.

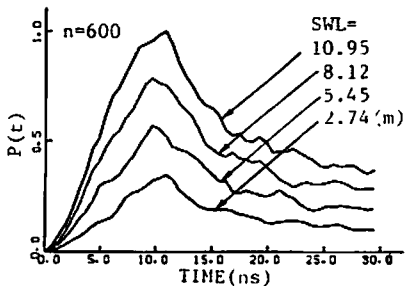


Fig. 8 The Mean Return Waveforms from Sea Surfaces with the Different Wavelengths.

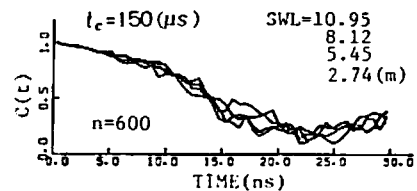


Fig. 9 The Correlation Coefficients of Return Pulses from Sea Surfaces with the Different Wavelengths.